IOP Conf. Series: Earth and Environmental Science **171** (2018) 012012 doi:10.1088/1755-1315/171/1/012012

Influence Analysis of Blade Fracture of Ducted Propellers of offshore platforms on Flow Field

L J Ou[1], **W Zhang** [2]

1 School of Civil Engineering and Transportation, South China University of Technology, Guangzhou 510640, China;
2 Guangzhou Maritime Safety Administration of the People's Republic of China, Guangzhou, 510700, China;

Abstract. The flow field of ducted propellers in viscous flow is analyzed and calculated with CFD technology, and the flow field and surface pressure distribution of the ducted propeller of offshore platforms with the fracture in different positions of a certain blade are simulated. Firstly, the geometrical models of the ducted propellers are established with UG software and put into the girding caved up by the Gambit. Then the numerical simulations are carried out with CFD, by which the surface pressure distribution of the ducted propellers in open water are calculated using Moving Mesh method. Lastly, the flow field characteristics of ducted propellers with the fracture in different positions of a certain blade are compared, and the result data are analyzed and summarized to gain flow field change laws. The results can be applied in project for reference.

1. Introduction

As special propellers, ducted propellers are widely applied to offshore platform dynamic positioning system. Because ducted propellers are less affected by the sea conditions changes outside and are protected by their ducts and also the ducts can improve the course stability significantly. Now ducted propellers are applied to lots of merchant vessels too. Numerical simulation has advantages of low-cost and short-cycle, and can obtain complete data and simulate the measurement of various data in practical operation process. CFD is widely applied to the numerical simulation of flow field. Because of its adaptability and accuracy00[3][4][5]. CFD gradually becomes an important tool in hydrodynamic research and its application areas have been gradually expanded. Through the analysis of ducted propellers by 3D unsteady CFD, the surface pressure distribution of ducted propellers can be investigated accurately. In the research and application of CFD, Su0 used the potential-based surface panel method numerically forecast unsteady performance of ducted propellers, and the predictions of hydrodynamics are high. But some error existed in surface pressure distribution of the duct surface circulation and pressure distribution of blade surface. In the prediction research of viscous CFD, Lu0 numerically simulated the open water performance of ducted propellers and the performance forecast accuracy with different grid models and turbulence models was compared and analyzed. It was concluded that k-ε turbulence model was more suitable for the numerical calculation of the open water performance of ducted propellers. Yao0 simulated the performance and flow field of ducted propellers with different Froude number using VOF. Li0 numerically researched the effects of tip clearance on duct propeller's hydrodynamic performance, and the results showed that thrust and moment decreased with increasing tip clearance, and tip clearance had obvious effect on the pressure distribution of blade surface near tip. Li0 numerically researched the influence of duct parameters on hydrodynamic performance and analyzed the influence law of length-diameter ratio, contraction coefficient and

dilatation coefficients on hydrodynamic performance. Li0 analyzed the PIV experimental data of propeller tail vortex field, including velocity distribution of trailing vortex area, trailing vortex structure, velocity deficit and eddy piece of layered and so on.

At present the numerical simulation methods of hydrodynamic performance of ducted propellers with CFD apply maturely already, so the flow field of the ducted propeller of offshore platforms is simulated using numerical forecast method with CFD in this article.

2. Computational Model and Method

2.1. Governing Equations and Numerical Methods

The relative rotation motion between the ducted propeller blade and the duct can be considered as the 3D unsteady flow of incompressible fluid, so it can be represented with the Reynolds-averaged momentum equation:

$$\frac{\partial}{\partial t}(\rho u_i)+\frac{\partial}{\partial x_j}(\rho u_i u_j)=-\frac{\partial p}{\partial x_i}+\frac{\partial p}{\partial x_j}[\mu(\frac{\partial u_i}{\partial x_j}+\frac{\partial u_j}{\partial x_i}-\frac{2}{3}\delta_{ij}\frac{\partial u_l}{\partial x_l})]+\frac{\partial}{\partial x_j}(-\rho\overline{u_i'u_j'}) \tag{1}$$

Where, ρ is fluid density, and $-\rho\overline{u_i'u_j'}$ is Reynolds stress. According to the eddy viscosity assumption by Boussinesq, the relationship between Reynolds stress and average velocity gradient is established, and that is:

$$-\rho\overline{u_i'u_j'}=\mu_t(\frac{\partial u_i}{\partial x_j}+\frac{\partial u_j}{\partial x_i})-\frac{2}{3}(\rho k+\mu_t\frac{\partial u_i}{\partial x_i})\delta_{ij} \tag{2}$$

Where, μ_t represents turbulent viscosity, and it is a function of turbulent kinetic energy k and turbulent dissipation rate ε.

The unsteady turbulent used in this article is calculated with the RNG *k-ε* double equation model and the renormalization group keeps the Reynolds average equation closed, and that is:

$$\rho\frac{Dk}{Dt}=\frac{\partial}{\partial x_j}(\alpha_k\mu_{eff}\frac{\partial k}{\partial x_j})+G_k+G_b-\rho\varepsilon-Y_M \tag{3}$$

Where, G_k is turbulent kinetic energy generated by gradient change, and G_b is turbulent kinetic energy produced by buoyancy change.

$$\rho\frac{D\varepsilon}{Dt}=\frac{\partial}{\partial x_j}(\alpha_\varepsilon\mu_{eff}\frac{\partial\varepsilon}{\partial x_j})+C_{1\varepsilon}\frac{\varepsilon}{k}(G_k+C_{3\varepsilon}G_b)-C_{1\varepsilon}\rho\frac{\varepsilon^2}{k}-R \tag{4}$$

With the amendment of turbulent viscosity in RNG *k-ε* double equation model compared with standard *k-ε* model, rotation and swirling flow in average flux are considered, and the model can hand the flow with high strain rate and large streamline deflection, so it is more suitable to hand the complex flow with the high speed rotating ducted propeller. The wall function is used in the near wall region.

Two-order implicit time marching method is applied in the separated solver to calculate the unsteady turbulent, and the standard law of wall is applied to treat the wall. Governing equations are dispersed in time and space. The finite volume method is used in space discretization transforming the governing equations to calculable algebraic equations. The finite volume method integrates governing equations on every calculating element, dispersed equations show flow filed parameters on every calculating element. Time discretization consists of all the integration of each element in different equations on time in a time step. The pressure term is dispersed with two-order central difference scheme, while others are dispersed with two-order upwind scheme.

2.2. Computational Modeling

2.2.1. Geometric model of the ducted propeller. Main dimensions and parameters of the ducted propeller: diameter $D=2.000$ meters; pitch ratio $H/D=0.900$; area ratio $A_Z/A=0.700$; hub diameter ratio $d_0/D=0.167$; blade number $Z=4$; back rake $\varepsilon=0$; stirring paddles $Ka4-70$. The propeller section type is 19A, the chord length is 1.00 meter, the distance Δ between the blade

and the duct is 4.0 millimeters, and the inside radius of the draft tube is 1.004 meters. The geometric model of the duct propeller is shown in Figure 1. In order to research the hydrodynamic performance of the ducted propeller with blade fractured, the CFD computational model of the ducted propeller with the fracture at different positions 0.9R, 0.8R, 0.7R, 0.6R, 0.5R of a certain blade, shown in Figure 2,is set to be calculated, compared, analyzed and researched.

The monitoring points are set to simulate the signal extracting of pressure sensors to get the fluctuating pressure of duct wall. By extracting the average pressure in the local region, the pressure variation values of the monitoring points are obtained. And real-time pressure values of the monitoring points are recorded with calculation to simulate the pressure sensors.

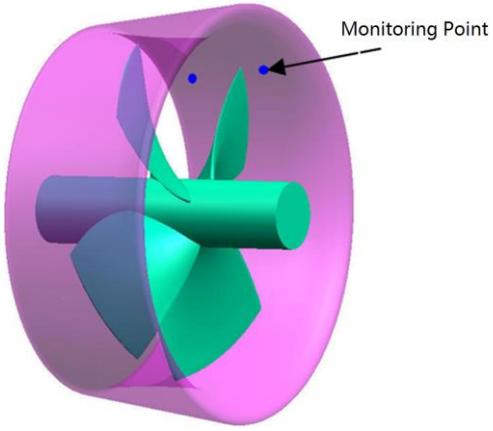

Figure 1. model of ducted propeller (monitoring points).

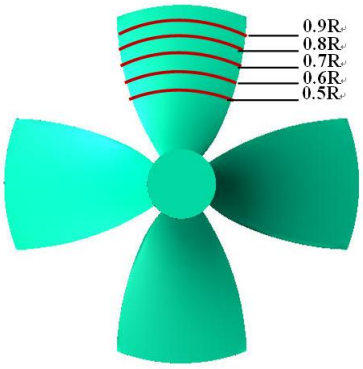

Figure 2. model of ducted propeller with the fracture at different positions.

2.2.2. Computing domain and mesh generation. The computational domain is cylindrical, and the radius R_a is 4 meters. The distance between the front of the computational domain and the propeller disk L_f is 4 meters, while the distance between the end of the computational domain and the propeller disk L_r is 6 meters. Mesh generation is the most important part in CFD simulation and one of key factors that have effect on simulation accuracy and efficiency. Over-sparseness grids result in inaccuracy, while over-density results in the increase of the amount and non-convergence of calculation. When meshing the interior computational domain, "Function{start size 12, growth size 1.4 size limit 20}" is a function defined in order to mesh the propeller tip and the domain with large curvature. The mesh generation of the interior computational domain is showed in Figure 3, and the mesh is 611 000. The mesh generation of the exterior computational domain is showed in Figure 4, and the mesh is 586 000. The data of the interior and exterior computational domain is exchanged through interface, which is meshed by regular grids.

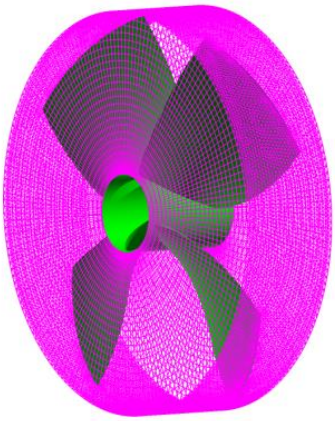

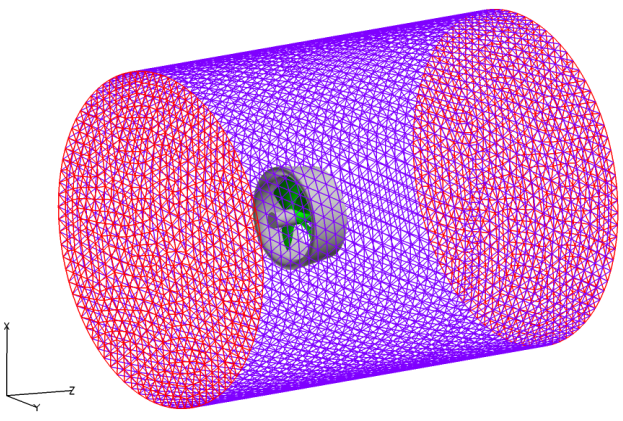

Figure 3. mesh generation of the interior computational domain.

Figure 4. mesh generation of the exterior computational domain

2.2.3. Boundary conditions. In the open water calculation of the ducted propeller, the whole computational domain is in rotation motion relative to some reference frame, and there is no mutual interference around.so MRF model can be used. Velocity inlet boundary conditions are set at the inlet boundary, and velocity components of the uniform inflow are set. The outflow velocity and pressure are unknown before the flow problem is solved, so mass flow inlet boundary conditions are set at the outlet boundary while the cylindrical surface is set as wall and no slip solid wall condition is set at wall. The fluid in the interior computational domain is using MRF model and rotates about axes with the angular velocity 5 revolutions per second (RPS) in the open water calculation of the ducted propeller.

3. Analysis of Duct Inner Wall Fluctuating Pressure and Flow Field Changes of Ducted Propellers with Blade Fractured

3.1. Analysis of Duct inner Wall Fluctuating Pressure of Ducted Propellers with Blade Fractured

Working Propellers are simulated through 3D unsteady calculation. With the duct inner wall fluctuating pressure of normal ducted propellers and the ones with blade fractured, pressure fluctuating graphs are obtained. Due to space limitations, pressure fluctuating graphs of monitoring points of normal ducted propellers and the ones with the fracture at different positions 0.9*R*, 0.8*R*, 0.7*R*, 0.6*R*, 0.5*R* of a certain blade are shown in Figure 5-8, respectively.

In the CFD, the rotation speed of the ducted propeller is 5r/s, which means the period is 0.2s, and the frequency is 5Hz and blade frequency is 20Hz.The results show that the duct inner wall fluctuating pressure of monitoring points varies periodically. The current of fluctuating pressure of normal ducted propellers is sin wave-form, and the change frequency is the same with blade frequency. The current of fluctuating pressure of ducted propellers with the fracture at different positions is deformed sin wave-form, and the change frequency is the same with rotation period of ducted propellers. The more fracture is, the more deformity of the current of fluctuating pressure is.

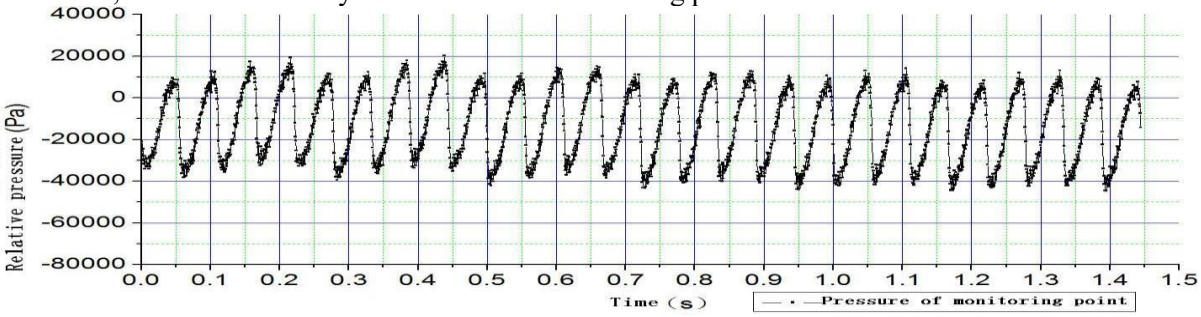

Figure 5. Pressure fluctuating graphs of normal ducted propellers.

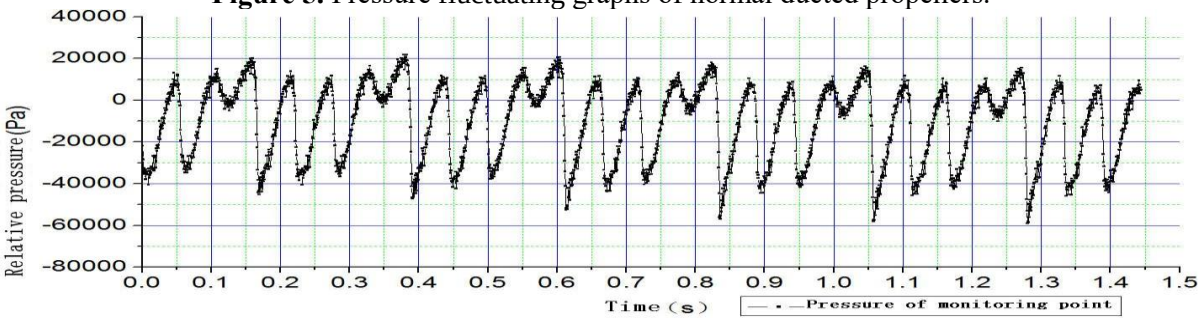

Figure 6. Pressure fluctuating graphs of ducted propellers with the fracture at 0.9R.

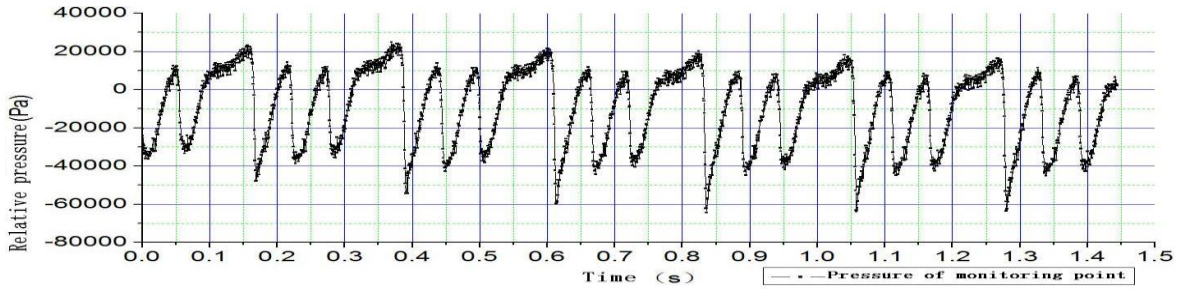

Figure 7. Pressure fluctuating graphs of ducted propellers with the fracture at 0.7R.

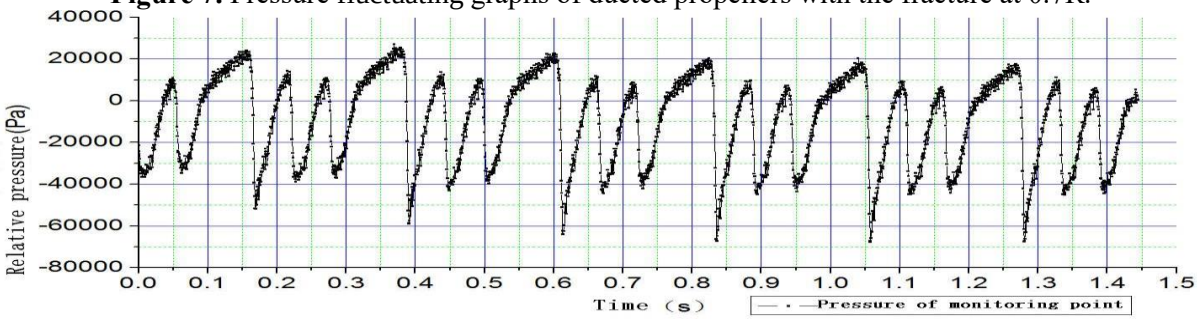

Figure 8. Pressure fluctuating graphs of ducted propellers with the fracture at 0.5R.

3.2. Influence Analysis of Blade Fracture of Ducted Propellers on Flow Field

To study the influence of blade fracture of ducted propellers, the flow field characteristics of normal ducted propellers and the ones with the fracture at different positions 0.7R and 0.5R are analyzed. The pressure of cross section of flow field at computational domain *Z*=3m, *Z*=0m, *Z*=-2.5m, *Z*=-5.5m is obtained, and the change law is compared and analyzed.

with ducted propellers fractured at different positions 0.7*R* and 0.5*R* ,the pressure distribution of cross section of flow field at computational domain *Z*=3m, *Z*=0m, *Z*=-2.5m, *Z*=-5.5m is shown in Figure 9,10 and 11,while the average relative axially pressure of flow field is shown in Figure 12.

From Figure 9, 10, 11, it is known that the suction of the inflow flow field displays a symmetrical distribution in normal working condition. The eccentric phenomenon of suction of the inflow flow field of ducted propellers appears when blade fractured. Stress nephograms show that the eccentricity lags behind the blade fracture position, which results from viscosity and lag of the flow. In normal working condition, the pressure of the trailing of ducted propellers displays a symmetrical distribution. The pressure of the trailing of ducted propellers with blade fractured displays an unsymmetrical distribution and eccentric phenomenon, which is affected by the fracture blade.

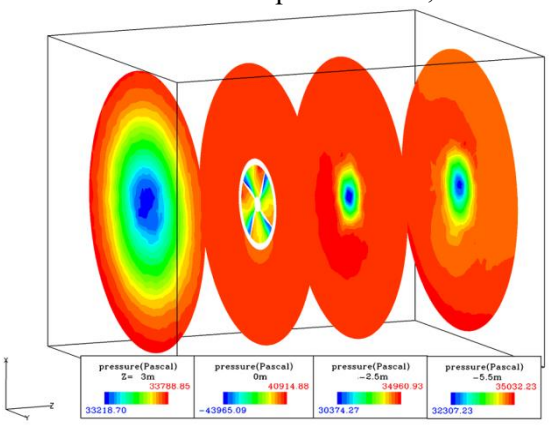

Figure 9. Stress nephograms in normal working condition.

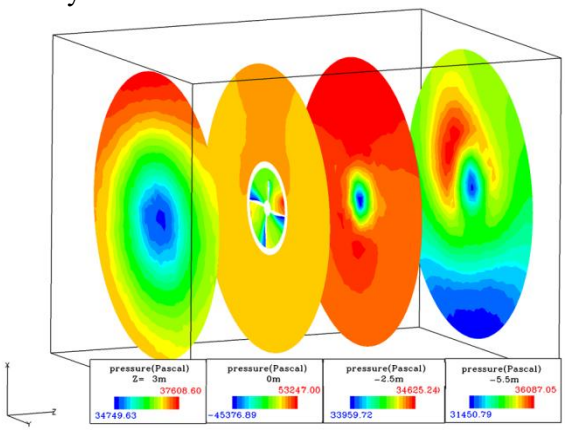

Figure 10. Stress nephograms in normal working condition of ducted propellers with the fracture at 0.7R.

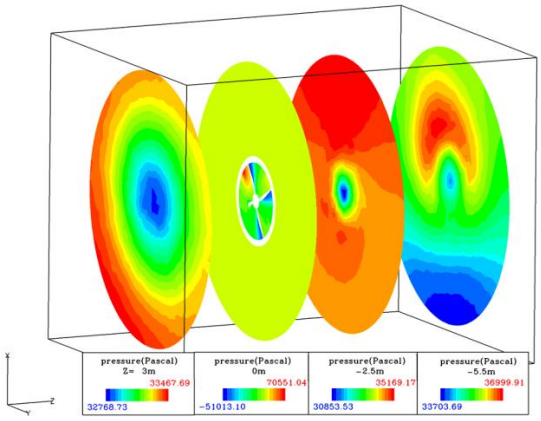

Figure 11. Stress nephograms in normal working condition of ducted propellers with the fracture at 0.5R.

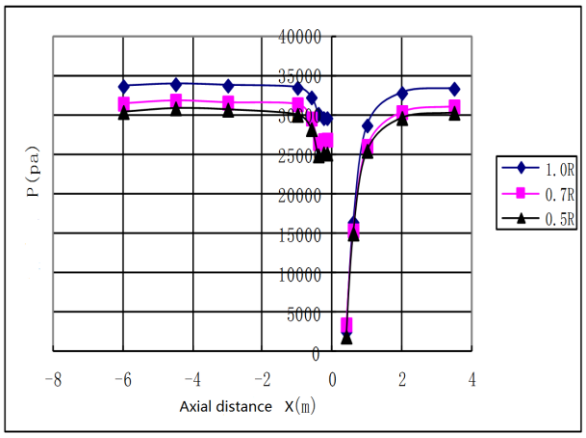

Figure 12. Comparison of pressure of normal ducted propellers and ones with the fracture at 0.7R and 0.5R.

4. Conclusions

(1) The results show that the duct inner wall fluctuating pressure of monitoring points varies periodically. The current of fluctuating pressure of normal ducted propellers is sin wave-form, and the change frequency is the same with blade frequency. The current of fluctuating pressure of ducted propellers with the fracture at different positions is deformed sin wave-form, and the change frequency is the same with rotation period of ducted propellers. The more fracture is, the more deformity of the current of fluctuating pressure is.

(2) The suction of the inflow flow field displays a symmetrical distribution in normal working condition. The eccentric phenomenon of suction of the inflow flow field of ducted propellers appears when blade fractured. Stress nephograms show that the eccentricity lags behind the blade fracture position, which results from viscosity and lag of the flow. In normal working condition, the pressure of the trailing of ducted propellers displays a symmetrical distribution. The pressure of the trailing of ducted propellers with blade fractured displays an unsymmetrical distribution and eccentric phenomenon, which is affected by the fracture blade.

(3) The pressure along the inflow of working flow field of ducted propellers is analyzed and it is found that the pressure of suction surface changes suddenly and the suction reaches maximum and the pressure of pressure surface recovers and increases. So there is pressure difference between the blade of ducted propellers and acting force in the opposite direction of inflow forms, which means the working principle of ducted propellers.

5. References

[1] X M Feng and F M Chen and R Q Cai 2006*Calculation of Propeller Open Water Performance by CFD Soft*ware FLUENT(China: SHIP AND BOAT)

[2] C Wang and S Huang and X S Xie 2008 *Hydrodynamic performance prediction of some propeller based on CFD* (China: JOURNAL OF NAVAL UNIVERSITY OF ENGINEERING)

[3] H Xu and J S Ma 2017 *CFD-based numerical study on the hull-rudder hydrodynamic interaction* (China: CHINESE JOURNAL OF HYDRODYNAMICS 32(3): 273-281)

[4] J Hu and N Wang and Y Hu 2017 *Numerical study on the hydrodynamic performance of ducted propellers* (China: JOURNAL OF HARBIN ENGINEERING UNIVERSIY 38(6): 815-821)

[5] X F Xue and T H Yan and B He 2017 *Modeling and Hydrodynamic Performance Analysis of MAU Propeller* (China: SHIP ENGINEERING 38(1): 38-42)

[6] Y M Su and Y B Liu and H L Shen 2012 *Surface Panel Method-Based Numerical Calculation for Predicting Ducted Propeller Performances* (China: JOURNAL OF HUAZHONG UNIVERSITY OF SCIENCE AND TECHNOLOGY.NATURE SCIENCE40(8): 57-61)

[7] X J Lv and Q D Zhou and G Ji and Y C Pan and B Fang 2010 *Prediction sand Comparison of Open Water Performance of Ducted Propeller* (China: JOURNAL OF NAVAL UNIVERSITY OF ENGINEERING 22(1): 24-30)
[8] Z Q Yao and W Chen 2011 *Numerical Analysis of Viscous Flow Field Around Ducted Propeller Considering Gravity* (China: JOURNAL OF JIANGSU UNIVERSITY OF SCIENCE AND TECHNOLOGY2 5(1): 1-3)
[9] J B Li 2010 *Influences of Tip Clearance on the Performance of Ducted Propeller*(China: SHIP AND OCEAN ENGINEERING 39(3): 36-39)
[10] C L and Y H Xie and L J Wang 2012 *Influence of Duct Parameters on the Hydrodynamic Performance of the Ducted Propeller* (China: SHIP AND BOAT 23(5): 17-22)
[11] G N Li and J Zhang and Z H Chen and Y H Xie 2011 *Propeller Trailing Vortex Analysis Based on PLV Experimental Data*(China: JOURNAL OF SHIP MECHANICS 15(10): 1110-1114)

Acknowledgement
This article is funded by the open project (NO.1605) of the country's key ocean engineering laboratory (Shanghai Jiao Tong University).